

Extending the Upper-Passband Range in Planar Bandstop-Type Transversal Filtering Sections

Roberto Gómez-García
Dpt. Signal Theory & Communications
University of Alcalá
Alcalá de Henares, Spain
roberto.gomez.garcia@ieeee.org

Li Yang
Dpt. Signal Theory & Communications
University of Alcalá
Alcalá de Henares, Spain
li.yang@uah.es

Abstract—A class of generalized two-path stepped-impedance-line signal-interference transversal filtering section (TFS) for bandstop applications is reported. By avoiding the frequency-periodic behavior intrinsic to its classic uniform-impedance-line bandstop TFS counterpart through the use of stepped-impedance lines in its electrical paths, a broadened upper-passband range is attained in this novel approach of bandstop TFS. This is achieved while maintaining the same filtering performance for the main stopband as in its associated conventional bandstop TFS, which suffers from the generation of odd-numbered-harmonic spurious rejected bands as design drawback. An optimization-based design example of an extended-upper-passband stepped-impedance-line bandstop TFS is shown for validation purposes, from which a 1-GHz microstrip prototype is experimentally developed and tested.

Index Terms—Bandstop filter (BSF), microstrip filter, microwave filter, planar filter, signal-interference filter, stepped-impedance line, transmission zero (TZ), transversal filtering section (TFS).

I. INTRODUCTION

Microwave bandstop filters (BSFs) are fundamental high-frequency components to assure the operational robustness of the RF transmitter and receiver front-ends by mitigating undesired spurious and out-of-system interfering signals, respectively. Nevertheless, when implemented in distributed-element RF technologies, unwanted spurious rejected bands above the main stopband are generally produced, which may restrict the operational bandwidth of the entire RF system [1], [2]. These undesired spurious stopbands are attributable to the frequency-periodic behavior of the transmission-line elements in classic planar BSF schemes or to the presence of upper modes in 3-D/waveguide BSF realizations [3], [4]. As a result, different RF design techniques to further enlarge the upper-passband range in microwave BSFs have been reported, with special emphasis on planar technologies. For example, in [5] and [6], stepped-impedance transmission-line segments are used in planar stub-loaded and three-coupled-line BSF configurations, respectively, in order to shift the upper spurious stopbands to higher frequencies. On the other hand, in [7], several inter-resonator coupling paths are introduced in a planar BSF topology to convert the signal interactions occurring at the spurious frequencies from destructive- to constructive-type ones, so that the spurious stopbands are no longer generated.

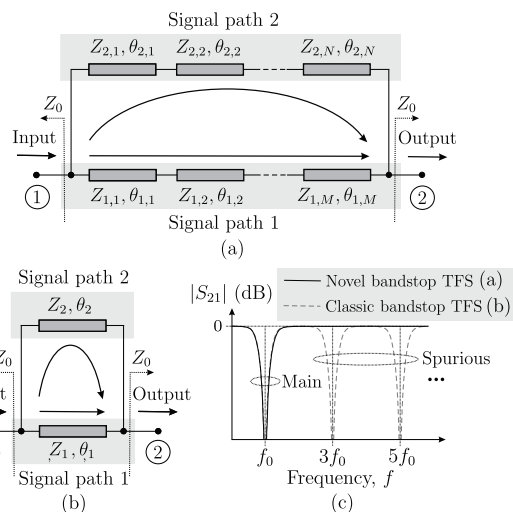


Fig. 1. (a) Novel stepped-impedance-line bandstop TFS with extended upper passband. (b) Classic bandstop TFS. (c) Operational principle in terms of conceptual power transmission response ($|S_{21}|$)— Z and θ variables refer to characteristic impedances and electrical lengths at the main-stopband center frequency f_0 , except Z_0 that is the reference impedance.

A novel strategy for the realization of planar BSFs with extended upper-passband range is presented. The proposed design technique is applied to a bandstop-type signal-interference transversal filtering section (TFS) shaped by two in-parallel transmission-line paths, where the main and spurious stopbands are created by means of destructive signal interference. Note that planar TFSs featuring a variety of filtering functionalities have been exploited in the past—e.g., bandpass [8], multi-passband [9], lowpass [10], and bandstop ones [11]–[15] as the main subject of this work—, but most of them suffer from spurious-band generation at harmonic frequencies due to its intrinsic spectral periodicity. In this paper, it is demonstrated that by replacing the uniform-impedance transmission-line paths of the conventional bandstop TFS by stepped-impedance-line ones, the upper spurious stopbands can be suppressed while keeping the same filtering behavior for the main stopband. As a result, an enlarged upper-passband range is obtained since the frequency-periodic behavior of the classic bandstop TFS is fully avoided through the action of the

stepped-impedance transmission-line paths. An optimization-based design example is shown in Section II to theoretically verify the principle. Furthermore, in Section III, a 1-GHz proof-of-concept microstrip prototype is developed and characterized for experimental-validation purposes.

II. STEPPED-IMPEDANCE-LINE BANDSTOP TFS

The circuit detail of the proposed stepped-impedance-line bandstop TFS is provided in Fig. 1(a). It is derived from its classic uniform-impedance-line bandstop TFS counterpart shown in Fig. 1(b) after dividing its two transmission-line paths into M and N line sub-segments, whose design parameters will be obtained through optimization. Specifically, for $\theta_1(f_0) = 90^\circ$, $\theta_2(f_0) = 270^\circ$, and $1/Z_1 + 1/Z_2 = 1/Z_0$ ($Z_1 \leq Z_2$), the conventional bandstop TFS in Fig. 1(b) exhibits a bandstop-type filtering response in which its main stopband is centered at f_0 and its spectrally-periodic upper stopbands are located at odd-numbered-harmonic frequencies—i.e., at $(2n+1)f_0$, $n \in \mathbb{N}$. For $Z_1 = Z_2 = 2Z_0$, all the stopbands have a double transmission zero (TZ) at the center frequency. On the other hand, for $Z_1 < Z_2$ while satisfying $1/Z_1 + 1/Z_2 = 1/Z_0$, the stopband bandwidth can be controlled by splitting the referred double TZ into two ones symmetrically located around the center frequency. Nevertheless, in all cases, the upper-passband range above the main stopband is contained within the spectral interval $(f_0, 3f_0)$ as a design restriction. This is conceptually illustrated in Fig. 1(c), which also shows how the suggested stepped-impedance-line bandstop TFS in Fig. 1(a) can overcome this limitation by breaking the spectral periodicity inherent to the classic bandstop TFS. This is because its building transmission-line sub-segments are no longer a multiple of 90° at f_0 in terms of electrical length.

Due to the large number design parameters involved in the devised stepped-impedance-line bandstop TFS, the derivation of a fully-analytical design methodology allowing to meet some prefixed specifications seems to be unfeasible. Thus, an optimization-based design approach that consists of the following steps is proposed instead for this novel bandstop TFS:

- 1) Design of a classic bandstop TFS from [12] satisfying the main-stopband requisites of minimum power-rejection level L_{min} within the frequency range (f_1, f_2) .
- 2) Division of the two transmission-line paths of the previously-designed classic bandstop TFS into M and N line subsegments, respectively, so that $\theta_{1,1} = \theta_{1,2} = \dots = \theta_{1,M} = \theta_1/M$, $\theta_{2,1} = \theta_{2,2} = \dots = \theta_{2,N} = \theta_2/N$, $Z_{1,1} = Z_{1,2} = \dots = Z_{1,M} = Z_1$, and $Z_{2,1} = Z_{2,2} = \dots = Z_{2,N} = Z_2$ as starting point of the modified bandstop TFS.
- 3) Optimization of the design parameters of the modified bandstop TFS to feature a minimum input-power matching level Γ_{min} within the frequency interval (f_3, f_4) .
- 4) If step 3) cannot be accomplished, increase M and N and return to step 1)—note that there is not robust criteria to find the optimum values for M and N .

By applying the previously-described algorithm, a theoretical design example of a stepped-impedance-line bandstop TFS

TABLE I
DESIGN VARIABLES OF THE OPTIMIZED BANDSTOP TFS

Stepped-impedance transmission-line path 1 ($M = 4$)					
i	$Z_{1,i}/Z_0$	$\theta_{1,i}(f_0)$	i	$Z_{1,i}/Z_0$	$\theta_{1,i}(f_0)$
1	2.284	22.4°	3	1.934	22.5°
2	2.028	22.2°	4	2.15	22.1°
Stepped-impedance transmission-line path 2 ($N = 12$)					
j	$Z_{2,j}/Z_0$	$\theta_{2,j}(f_0)$	j	$Z_{2,j}/Z_0$	$\theta_{2,j}(f_0)$
1	1.902	18.6°	7	1.652	23.7°
2	2.13	29°	8	2.448	23.7°
3	2.058	22.3°	9	1.626	19.2°
4	1.61	19.9°	10	1.994	26.9°
5	2.438	20°	11	1.958	21.4°
6	1.718	22.7°	12	1.752	21.3°

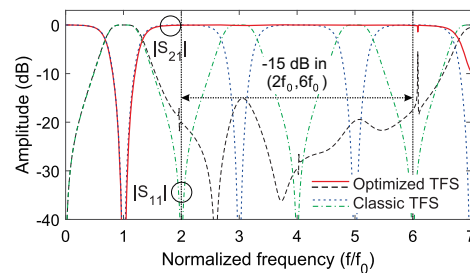


Fig. 2. Theoretical power transmission ($|S_{21}|$) and input-reflection ($|S_{11}|$) responses of the optimized stepped-impedance-line bandstop TFS with extended upper passband—the values for the design parameters are listed in Table I—compared to those of the classic bandstop TFS.

that avoids the creation of the first and second upper spurious stopbands at the locations $3f_0$ and $5f_0$, respectively, was carried out. Specifically, the following design specifications were imposed: $L_{min} = 20$ dB, $\Gamma_{min} = 15$ dB, $f_1 = 0.9f_0$, $f_2 = 1.1f_0$, $f_3 = 2f_0$, and $f_4 = 6f_0$. The values for the design parameters of this bandstop TFS example are listed in Table I. Its theoretical power transmission and input-reflection responses are compared in Fig. 2 with those of its classic bandstop TFS counterpart, thus proving the fulfilment of the prefixed upper-passband-enlargement requisite. Note also that this is done while slightly shortening the total electrical lengths for both transversal transmission-line paths—in particular, 89.2° and $268.7.5^\circ$ versus 90° and 270° at f_0 , respectively.

III. EXPERIMENTAL RESULTS

For practical-validation purposes, the stepped-impedance-line bandstop-type TFS example with extended upper stopband that was optimized in the Section II has been manufactured in microstrip technology and characterized. A reference-impedance level $Z_0 = 50 \Omega$ and a center frequency $f_0 = 1$ GHz were selected for its development, which results in a theoretical 20-dB-attenuation-referred absolute bandwidth of 200 MHz. For its implementation, a Rogers 4003C microstrip substrate with the following parameters was used: relative dielectric permittivity $\epsilon_r = 3.38$, dielectric thickness $H = 1.524$ mm, metal thickness $t = 17.8 \mu\text{m}$, and dielectric

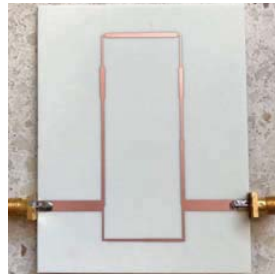
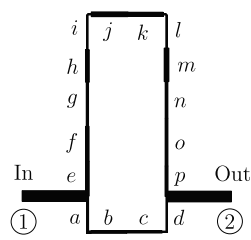


Fig. 3. Layout and photograph of the manufactured microstrip prototype of stepped-impedance-line bandstop TFS with extended upper passband (non-redundant dimensions, in mm—“ w ” stands for widths and “ l ” for middle lengths including bends when applicable but not considering T-junction regions: $w_{in} = w_{out} = 3.38$, $l_{in} = l_{out} = 20$, $w_a = 0.45$, $l_a = 10.87$, $w_b = 0.68$, $l_b = 11.16$, $w_c = 0.89$, $l_c = 11.28$, $w_d = 0.66$, $l_d = 10.07$, $w_e = 0.93$, $l_e = 7.93$, $w_f = 0.88$, $l_f = 15.08$, $w_g = 0.85$, $l_g = 11.52$, $w_h = 1.48$, $l_h = 10.58$, $w_i = 0.45$, $l_i = 11.28$, $w_j = 1.29$, $l_j = 11.08$, $w_k = 1.5$, $l_k = 11.57$, $w_l = 0.44$, $l_l = 11.96$, $w_m = 1.2$, $l_m = 10.23$, $w_n = 0.72$, $l_n = 13.91$, $w_o = 1.06$, $l_o = 11.01$, $w_p = 1.14$, and $l_p = 9.28$).

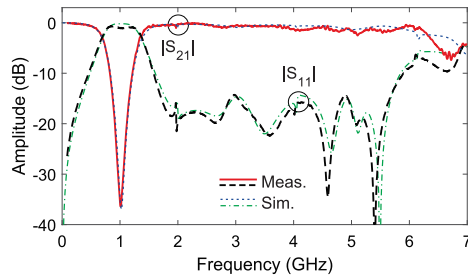


Fig. 4. Simulated and measured power transmission ($|S_{21}|$) and input-reflection ($|S_{11}|$) responses of the manufactured microstrip prototype of stepped-impedance-line bandstop TFS with extended upper passband.

loss tangent $\tan(\delta_D) = 0.0027$. The simulation and optimization processes of this bandstop TFS were carried out with the commercial electromagnetic-(EM)-software tool Ansys HFSS, whereas its measurements in terms of S -parameters were performed through an Agilent E8361A vector network analyzer.

The layout and a photograph of the constructed bandstop TFS prototype are shown in Fig. 3. A comparison between its simulated and measured power transmission and input-reflection responses is provided in Fig. 4. As can be seen, a fairly-close agreement between predicted and experimental results is obtained. The main measured characteristics of the fabricated bandstop TFS circuit for its main stopband are as follows: center frequency of 1.01 GHz, notch-depth level of 36.4 dB, and 20-dB-attenuation-referred absolute bandwidth equal to 203 MHz—i.e., of 20.1% in relative terms. The measured upper-passband range extends from 1.583 GHz to 5.895 GHz—i.e., 3.72:1 spectral ratio—for a minimum input-power-matching level of 10 dB, thus completely verifying the effectiveness of the proposed optimization-based BSF design methodology.

IV. CONCLUSION

The potential of using stepped-impedance transmission-line paths in bandstop-type TFSs to further extend their

upper-passband range has been demonstrated in this paper. This is achieved by breaking the spectral periodicity inherent to traditional uniform-line-impedance bandstop TFSs, which gives rise to spurious stopbands that are located at harmonic frequencies. An optimization-based design example has been shown, and subsequently manufactured in microstrip technology for a stopband center frequency of 1 GHz. It features an enlarged 10-dB-input-power-matching-level-referred upper-passband range up to ≈ 5.9 times the main-stopband center frequency, hence validating the engineered BSF principle.

ACKNOWLEDGMENT

This work was supported in part by the Spanish Ministry of Economy, Industry, and Competitiveness (State Research Agency) under Project TEC2017-82398-R and in part by the GOT ENERGY TALENT (GET) fellowship programme co-funded by the EU as part of the H2020-MSCA-COFUND programme (Grant Agreement number 754382).

REFERENCES

- [1] J.-S. Hong and M. J. Lancaster, *Microstrip Filters for RF/Microwave Applications*. New York, NY, USA: Wiley, 2001.
- [2] R. J. Cameron, C. M. Kudsia, and R. R. Mansour, *Microwave Filters for Communications Systems*, first ed. New York: Wiley, 2007.
- [3] J. A. G. Malherbe, “Wide-band bandstop filters with sub-harmonic stubs,” *IET Electron. Lett.*, vol. 47, no. 10, pp. 604–605, May, 2011.
- [4] J. R. Montejó-Garai, J. A. Ruiz-Cruz, J. M. Rebollar, and T. Estrada, “In-line pure-plane waveguide band-stop filter with wide spurious-free response,” *IEEE Microw. Wireless Compon. Lett.*, vol. 21, no. 4, pp. 209–211, Apr. 2011.
- [5] R. Levy, R. V. Snyder, and S. Shin, “Bandstop filters with extended upper passbands,” *IEEE Trans. Microw. Theory Techn.*, vol. 54, no. 6, pp. 2503–2515, Jun. 2006.
- [6] W. Tang and J.-S. Hong, “Coupled stepped-impedance-resonator band-stop filter,” in *IET Microw. Antennas Propag.*, vol. 4, no. 10, pp. 1283–1289, Sep. 2010.
- [7] A. C. Guyette, “Design of fixed- and varactor-tuned bandstop filters with spurious suppression,” in *40th Eur. Microw. Conf.*, Paris, France, Sep. 28–30, 2010, pp. 288–291.
- [8] R. Gómez-García and J.I. Alonso, “Design of sharp-rejection and low-loss wide-band planar filters using signal-interference techniques,” *IEEE Microw. Wireless Compon. Lett.*, vol. 15, no. 8, pp. 530–532, Aug. 2005.
- [9] R. Gómez-García, J.-M. Muñoz-Ferreras, and M. Sánchez-Renedo, “Microwave transversal six-band bandpass planar filter for multi-standard wireless applications,” in *2011 IEEE Radio Wireless Symp.*, Phoenix, AZ, USA, Jan. 16–19, 2011, pp. 166–169.
- [10] R. Gómez-García, M.-A. Sánchez-Soriano, M. Sánchez-Renedo, G. Torregrosa-Penalva, and E. Bronchalo, “Low-pass and bandpass filters with ultra-broad stopband bandwidth based on directional couplers,” *IEEE Trans. Microw. Theory Techn.*, vol. 61, no. 12, pp. 4365–4375, Dec. 2013.
- [11] M. K. Mandal and S. Sanyal, “Compact bandstop filter using signal interference technique,” *IET Electron. Lett.*, vol. 43, no. 2, pp. 110–111, Feb. 2007.
- [12] M. K. Mandal and P. Mondal, “Design of sharp-rejection, compact, wideband bandstop filters,” *IET Microw. Antennas Propag.*, vol. 2, no. 4, pp. 389–393, Jun./Jul. 2008.
- [13] M. Á. Sanchez-Soriano, G. Torregrosa-Penalva, and E. Bronchalo, “Compact wideband bandstop filter with four transmission zeros,” *IEEE Microw. Wireless Compon. Lett.*, vol. 20, no. 6, pp. 313–315, Jun. 2010.
- [14] Q.-X. Chu and L.-L. Qiu, “Sharp-rejection bandstop filter based on signal interference technique integrating with conventional open stubs,” in *2014 IEEE MTT-S Int. Microw. Symp.*, Tampa, FL, USA, Jun. 1–6, 2014, pp. 1–4.
- [15] R. Gómez-García, L. Yang, J.-M. Muñoz-Ferreras, and W. Feng, “Quasi-reflectionless signal-interference wide-band bandstop filters,” in *2019 IEEE MTT-S Int. Conf. Numer. Electromagn. Multiphys. Modeling Optim.*, Cambridge, MA, USA, May 29–31, 2019, pp. 1–4.